

1 **Title:** Memory drives the formation of animal home ranges: evidence from a reintroduction

2

3 **Authors:** Nathan Ranc<sup>1,2</sup>, Francesca Cagnacci<sup>1,2\*</sup> and Paul R. Moorcroft<sup>1\*</sup>

4

5 <sup>1</sup>Department of Organismic and Evolutionary Biology, Harvard University, 26 Oxford Street,  
6 Cambridge MA02138, USA.

7 <sup>2</sup>Department of Biodiversity and Molecular Ecology, Research and Innovation Centre,  
8 Fondazione Edmund Mach, Via E. Mach 1, 38010 San Michele all'Adige, Italy.

9 \*F. Cagnacci and P.R. Moorcroft and are co-senior authors.

10

11 **Corresponding Author:** Nathan Ranc (nathan.ranc@gmail.com)

12

### 13 **Abstract**

14 Most animals live in a characteristic home range, a space-use pattern thought to emerge from the  
15 benefits of memory-based movements; however, a general model for characterizing and predicting  
16 their formation in the absence of territoriality has been lacking. Here, we use a mechanistic  
17 movement model to quantify the role of memory in the movements of a large mammal reintroduced  
18 into a novel environment, and to predict observed patterns of home range emergence. We show  
19 that an interplay between memory and resource preferences is the primary process influencing the  
20 movements of reintroduced roe deer (*Capreolus capreolus*). Our memory-based model fitted with  
21 empirical data successfully predicts the formation of home ranges, as well as emerging properties  
22 of movement and revisits observed in the reintroduced animals. These results provide a quantitative  
23 framework for combining memory-based movements, resource preference and the emergence of  
24 home ranges in nature.

## 25 **Introduction**

26 Most animals live in home ranges – areas that are typically much smaller than their movement  
27 capabilities would otherwise allow<sup>1</sup>. The spatially-constrained nature of animal space-use has  
28 important implications for many ecological processes, including density-dependent regulation of  
29 population abundance<sup>2</sup>, predator-prey dynamics<sup>3</sup>, the spread of infectious diseases<sup>4</sup>, as well as for  
30 the design of conservation strategies<sup>5</sup>. Home ranges are pervasive throughout the animal  
31 kingdom, suggesting that they may provide fitness benefits in a wide range of ecological  
32 contexts, and originate from general biological mechanisms<sup>6</sup>. In territorial species, the emergence  
33 of a constrained space-use has been successfully characterized by analytical movement models  
34 based on conspecific avoidance<sup>3,7-9</sup>. However, a general model for predicting emergent patterns  
35 of space-use is still lacking for animals that form home ranges in the absence of territoriality or  
36 central place foraging.

37 In recent years, increasing attention has been devoted to the hypothesis suggesting that  
38 home ranges emerge from the foraging benefits of memory<sup>10,11</sup>. Theoretical studies have  
39 demonstrated the foraging advantages of memory over proximal mechanisms (e.g., area-restricted  
40 search and perception) in spatially-heterogeneous, predictable landscapes<sup>12-14</sup>. In turn,  
41 simulations have shown that memory-based movements can lead to the formation of stable home  
42 ranges<sup>15,16</sup>, and to non-territorial spatial segregation between individuals<sup>17</sup>. However, our  
43 understanding of how memory influences animal movement and resulting space-use patterns in  
44 nature is still in its infancy.

45 Optimal foraging experiments have provided evidence for the adaptive value of memory.  
46 For example, green-backed fire-crown hummingbirds (*Sephaniodes sephaniodes*) can achieve  
47 substantial energy gains by adjusting their visit frequency to the renewal dynamics of high-  
48 quality resources at memorized locations<sup>18</sup>. At larger spatial scales, mechanistic models based on

49 telemetry data have shown that animals are capable of memorizing the location and profitability  
50 of resources<sup>19,20</sup>. For example, roe deer (*Capreolus capreolus*) rely on memory, and not  
51 perception, to track the dynamics of resource availability within their home range<sup>21</sup>. Whether  
52 mechanistic movement models parametrized with empirical data can capture the spatial patterns  
53 of animal home ranges in nature remains, however, largely unanswered.

54         Most studies of animal home range movements have been conducted on resident animals  
55 whose experience and knowledge of the surrounding environment is already well-developed at  
56 the onset of monitoring<sup>19,20,22,23</sup>. This is problematic when studying the effects of memory  
57 because animals are utilising knowledge obtained prior to the observation period, which has been  
58 proposed as the reason for discrepancies between memory-based movement model predictions  
59 and observed space-use patterns<sup>22</sup>. One approach to address this challenge is to examine the  
60 process of home range formation (also referred to as emergence) when animals have been  
61 introduced into a novel environment<sup>11</sup>, where it can be reasonably assumed that the animals have  
62 no existing memories of the local environment.

63         In this study, we elucidate the role of memory in the movements of animals by analysing  
64 the process of home range formation of individuals reintroduced into a novel environment. Our  
65 results show how the interplay between memory and resource (landscape attributes) preferences  
66 gives rise to observed patterns of home ranges. Specifically, we fit an individual-based, spatially  
67 explicit movement model to the observed trajectories of European roe deer reintroduced into the  
68 Aspromonte National Park (Calabria, Italy), where the species had previously been extirpated.  
69 This experimental system is ideally-suited to the study of the biological determinants of home  
70 ranging behaviour for three reasons. First, because roe deer were released into a novel  
71 environment, as noted above, the theoretical challenge of how to initialize memory at the  
72 beginning of the simulation is essentially side-stepped. Second, because roe deer are solitary<sup>24</sup>,

73 their movements are expected to be primarily based on individual information rather than group  
74 decision making<sup>25</sup>. Third, because roe deer population was being re-established, animal density  
75 was low throughout the study, therefore limiting the influence of intraspecific competition on  
76 individual movements and space-use.

77 Roe deer were fitted with GPS telemetry collars and monitored from their release into the  
78 study area till the collars ceased functioning (n =17 individuals; see *Methods*). We analysed the  
79 biological processes underlying roe deer movements (n = 17,136 six-hour movement steps) using  
80 a redistribution kernel<sup>9,20,26</sup>. The model characterizes the probability that a given individual  
81 moves from its current position to any location in the landscape as a function of motion capacity,  
82 and a weighting function including resource preferences and memory. Building up on earlier  
83 work<sup>15-17</sup>, memory was represented as a bi-component mechanism: a *reference memory* encoding  
84 long-term attraction to previously visited locations, and a *working memory*, which accounts for a  
85 short-term avoidance of recently visited locations (for example, due to local resource  
86 depletion<sup>15</sup>). The dynamics of both memory components are governed by their respective  
87 learning and decay rates, and associated spatial scale.

88 We hypothesized that the interplay between memory and resources was the primary driver  
89 underlying roe deer movements (H1). To this end, we fitted two competing movement models: (i)  
90 a *resource-only* model ( $M_{res}$ ) in which roe deer movement was only influenced by resource  
91 preferences (which in this case corresponds to landscape attributes such as slope, tree cover and  
92 landcover categories; sensu <sup>27</sup>). (ii) a *memory-based* model ( $M_{mem.res}$ ) in which movement was  
93 governed by the interplay between memory and resource preference (sensu <sup>26</sup>). Following on our  
94 previous work that examined memory dynamics in an experimental setting<sup>21,28</sup>, we predicted that  
95 the empirical movement data would provide a higher support to the memory-based model than its

96 resource-only counterpart (P1.1). In addition, we predicted that, overall, roe deer would strongly  
97 select for previously visited locations (P1.2).

98 We further hypothesized that the interplay between memory and resource preferences can  
99 lead to formation of home ranges, as observed in the reintroduced roe deer (Cagnacci *et al.* in  
100 prep; H2). To this end, we compared the emerging movement and space-use properties of  
101 trajectories simulated from the parametrized redistribution kernels with those from the empirical  
102 roe deer movements. Accordingly, we predicted that, in contrast with the resource-only model,  
103 the simulations from the memory-based model would lead to spatially-constrained movements  
104 (P2.1) with a high prevalence of acute turning angles (P2.2). In addition, we predicted that  
105 memory-based movements would be characterized by a high number of revisitations (also  
106 referred to as movement recursions<sup>29</sup>; P2.3). Further details on the mathematical formulations of  
107 the redistribution kernel and on the movement simulations can be found in the *Methods* section.

108

## 109 **Results**

### 110 *Biological drivers of reintroduced roe deer movements*

111 The movement model that included both memory and resource preferences ( $M_{\text{mem:res}}$ ) had  
112 overwhelmingly stronger support compared to the resource-only model ( $M_{\text{res}}$ ;  $\Delta\log\text{-likelihood} = -$   
113  $8684$ ;  $\Delta\text{df} = -6$ ;  $\Delta\text{AIC} = 17355$ ;  $p\text{-value} < 0.001$ ; Table 1; P1.1 supported). Memory was a key  
114 biological process underlying the movements of reintroduced roe deer (most influential variable;  
115 Table 1; P1.1 supported). The importance of memory was primarily due to the effects of  
116 reference memory ( $\Delta\text{AIC} = 1278$  when working memory was removed, compared to  $\Delta\text{AIC} =$   
117  $17355$  when both working and reference memory were removed; see Table 1). With respect to  
118 reference memory, the spatial scale of learning was most influential ( $\Delta\text{AIC} = 7444$  if learning

119 occurred only on the visited locations i.e.,  $\lambda_R = \infty$ ), followed by learning rate ( $\Delta AIC = 3434$  if  
120 learning was immediate i.e.,  $l_R = 1$ ) and decay rate ( $\Delta AIC = 2631$  if there was no memory decay  
121 i.e.,  $\delta_R = 0$ ).

122  
123 Roe deer acquired memories of visited locations, with the learning curve reaching half its  
124 maximum value (i.e., memory = 0.5) after 7.9 days for reference memory ( $l_R = 0.0217 \text{ 6h}^{-1}$ ; see  
125 Fig. 1a for confidence intervals), and after 8.4 days for working memory ( $l_W = 0.0204 \text{ 6h}^{-1}$ ).  
126 Spatially, information was gained beyond the visited locations: reference memory learning  
127 decayed with distance to half its maximum value at 14.3 m ( $\lambda_R = 0.0485 \text{ m}^{-1}$ ; meaning that at 25  
128 m distance, learning was approximately 30 % that of the amount of memory acquired on the  
129 visited spatial location). Working memory learning declined to half its maximum value at 8.1 m  
130 ( $\lambda_W = 0.0855 \text{ m}^{-1}$ ; meaning that the learning rate at 25 m distance was approximately 12 % that  
131 of the visited location). Temporally, reference memory decayed with time since last visit with a  
132 half-life ( $t_{1/2}$ ) of 9.5 days ( $\delta_R = 0.0182 \text{ 6h}^{-1}$ ) while working memory decay was nearly  
133 instantaneous ( $t_{1/2} < 1 \text{ h}$ ;  $\delta_W = 0.99 \text{ 6h}^{-1}$ ).

134 The combined effect of memory dynamics and of the intrinsic component of resource  
135 preference (i.e., the attraction of locations in absence of memory;  $\varepsilon = 6.94 \times 10^{-4}$ ; Fig. 1b) led to a  
136 very strong selection for previously-visited locations (P1.2 supported). Specifically, the first visit  
137 of a given location resulted in a 31.6-fold increase in its attraction, and a 10.1-fold increase on the  
138 adjacent locations (Fig. 2a).

139 Roe deer movements were also influenced by their resource preferences (Fig. 1b;  $\Delta AIC =$   
140 304 when resource preferences were null i.e.,  $\beta_1 : \beta_6 = 0$ ; Table 1). Roe deer preferred  
141 intermediate slopes (Fig. 2b), with peak preference at eight degrees (most influential resource;

142  $\Delta\text{AIC} = 138$  when  $\beta_1 = \beta_2 = 0$ ; Table 1). Roe deer preference for tree cover was characterized  
143 by slight qualitative differences between models: preference for intermediate tree cover (a clear  
144 peak at 57%) in the resource-only model, and for intermediate and high levels of tree cover (a  
145 broad peak at 73%) in the memory-based model (Fig. 2c;  $\Delta\text{AIC} = 34$  when  $\beta_3 = \beta_4 = 0$ ; Table  
146 1). In addition, roe deer strongly preferred reforested areas and avoided agricultural areas (Fig.  
147 3c;  $\Delta\text{AIC} = 83$  when  $\beta_6 = 0$  and  $\Delta\text{AIC} = 59$  when  $\beta_5 = 0$ , respectively; Table 1). For all  
148 evaluated resources, preferences had a lower effect size for the memory-based model than for the  
149 resource-only model (Fig. 1b).

150 Roe deer motion capacity greatly differed between the two competing movement models.  
151 The resource-only model characterized the movement distances between six-hour relocations as a  
152 heavy-tailed Weibull distribution (shape parameter  $\kappa_S = 0.79$ ; decay rate parameter  $\lambda_S = 0.0078$ ;  
153 Fig. 1c), with a corresponding mean step length of 147.0 m. In contrast, the memory-based model  
154 indicates a nearly 3-fold larger motion capacity ( $\kappa_S = 1.02$ ;  $\lambda_S = 0.0024$ ) corresponding to a mean  
155 step length = 409.4 m). The value of the shape parameter  $\kappa_S$  being close to one implies that the  
156 step length distribution can be simplified to a negative exponential with a relatively small  
157 decrease in model accuracy ( $\Delta\text{AIC} = 4$  if  $\kappa_S = 1.00$ ; Table 1). Step length decay rate was,  
158 however, a highly influential parameter ( $\Delta\text{AIC} = 4945$  when compared with a resource-selection  
159 type movement kernel which assumes that roe deer spatial locations independently of their  
160 proximity i.e.,  $\lambda_S = 0$ ; Table 1).

161

### 162 *Emergent space-use and movement properties*

163 Most reintroduced roe deer settled into a constrained space (i.e., formation of a home range) as  
164 shown visually by the spatial concentration of their movements (Fig. 3b). The movement

165 simulations from the resource-only model were typical of a random walk (technically, an  
166 inhomogeneous random walk due to the effects of resource preferences; Fig. 3a). In contrast, the  
167 memory-based model captured the characteristic space-use behaviour observed in released roe  
168 deer (Fig. 3c; see Supplementary S1 for additional movement trajectories).

169 The visual differences in patterns of movement behaviour seen in Figure 3 were  
170 characterized and quantified by examining the temporal trends in net squared displacement  
171 (NSD) with time since release (Fig. 4). The resource-only model did not capture the observed  
172 spatially-restricted movements of the released roe deer, with no saturation in the NSDs of  
173 individuals (Fig. 4a), and a linear increase of the mean NSD across individuals (compare the solid  
174 red line on Fig. 4b with the red line and grey shaded area in Fig. 4a). In contrast, the predictions  
175 of the memory-based movement model were consistent with the temporal trends in the observed  
176 movements of the released animals as demonstrated by the occurrence of prolonged plateaus in  
177 the NSD of individual animals (Fig. 4c; P2.1 supported), and the fact that the observed mean  
178 NSD across individuals is within the bounds of the predictions of the memory-based movement  
179 model (compare the solid red line on Fig. 4b with the grey area on Fig. 4c).

180 Both the resource-only and memory-based models had step length distributions that  
181 closely matched the observations (Fig. 5a,b). The memory-based model more accurately  
182 characterized the observed median step length while the resource-only model better captured its  
183 mean (median step lengths of 55.9, 75.0 and 50.0 m; means of 141.1, 135.2 and 105.5 m for  
184 observed movements, resource-only simulations and memory-based simulations, respectively). In  
185 contrast, the two models differed greatly in their ability to reproduce the observed patterns of  
186 turning angles: the resource-only model showed a uniform circular distribution of turning angles  
187 (Fig. 5c) whereas the memory-based model captured the high density of acute turning angles (in



188 the vicinity of  $-\pi$  and  $+\pi$ ), that are characteristic of observed roe deer movements (Fig. 5d; P2.2  
189 supported).

190 Observed roe deer movement behaviour was characterized by frequent revisits: 33.8% of  
191 the utilized locations (spatial scale = 25 x 25 m) were visited twice or more. The simulations  
192 from the resource-only model, however, had very few revisits – only 4.5% spatial locations were  
193 revisited – leading to a large mismatch with the revisitation patterns of observed trajectories (Fig.  
194 6a). In contrast, the memory-based simulations were characterized by many revisits: 35.2% of the  
195 locations were revisited (P2.3 supported). The revisitation patterns of the memory-based model  
196 were highly similar to those of the observed roe deer movements (Fig. 6b), albeit with a slight  
197 tendency to underestimate the number of locations with few revisits (i.e., less than five), and to  
198 overestimate those with many revisits (especially above 20). Consistent with these patterns in the  
199 number of revisits, the memory-based model also captured the observed patterns of time since  
200 last visit more accurately than the resource-only model (compare Figs 6c and 6d, respectively).

201

## 202 **Discussion**

203 The past two decades have seen remarkable advances in the ability to monitor animal  
204 movements<sup>30</sup>, and the development of ever more complex and comprehensive mechanistic  
205 movement models. However, our understanding of the underlying biological determinants of  
206 home ranges – the most prevalent space-use pattern observed in animals – has been relatively  
207 limited<sup>6,11,31</sup>. In this study, we evaluated how memory-based movements can predict the  
208 formation of home ranges in nature by parametrizing a mechanistic movement model with  
209 empirical data from animals reintroduced into a novel environment. We found that an interplay  
210 between memory and resource preferences was the primary process influencing reintroduced roe  
211 deer movements (Fig. 2; H1), and that it led to the formation of characteristic home ranges, as

212 observed in the released individuals (Figs 3 and 4; H2; see also Cagnacci *et al.* in prep). To our  
213 knowledge, this is the first demonstration that a mechanistic movement model parametrized with  
214 empirical movement data can capture patterns of home range formation in a non-territorial  
215 species.

216 We found that the emergent properties of the memory-based movement model, as  
217 opposed to a resource-only movement model, were realistic and similar to the patterns observed  
218 in the reintroduced roe deer (Figs 3-5). First and foremost, the memory-based simulations gave  
219 rise to spatially-restricted movements, as shown by the saturation of individual net squared  
220 displacement with time since release (Fig. 4). In addition, the model successfully reproduced the  
221 heterogeneity and complexity of observed movement patterns, including long-distance  
222 explorations, multiple areas of concentrated use, and patterns of revisitation (Figs 3 and 6).

223 Two approaches can be used to study the underlying determinants of animal space-use<sup>32</sup>:  
224 analyses inferring underlying movement parameters that capture observed space-use patterns i.e.,  
225 pattern-oriented<sup>3,8,31,33,34</sup>, and analyses of individual movement trajectories to parametrise  
226 movement models<sup>20,23,35</sup>. In this study, we used the latter approach: characterizing the biological  
227 drivers of fine-scale behavioural decisions through the fitting of a mechanistic movement model  
228 to empirical trajectories, and subsequently evaluating resulting predictions of space-use  
229 properties. Although challenging, this approach is appealing because the space-use pattern itself  
230 is not fitted to data, but rather arises as an emergent property from the underlying movement  
231 process<sup>32,35</sup>.

232 Previous analyses have shown that memory influences the proximate behavioural  
233 decisions of free-ranging animals<sup>19,20,22,23</sup>. Our study extends these analyses in three major ways.  
234 First, we show that a movement model operating in a spatially continuous landscape not only  
235 accounts for the observed aggregate (population-level) patterns of space-use, but also yields

236 realistic patterns of individual space-use (Figs 3 and 4). Second, our empirical setting of animals  
237 reintroduced into a novel environment allowed us to avoid the problematic issue of how to  
238 initialize memory-based movement models<sup>19,20,23</sup> that has been invoked to explain the  
239 discrepancies between predicted and observed space-use patterns<sup>22</sup>. Third, as we discuss in more  
240 detail below, in addition to space-use patterns, the memory-based movement model captured  
241 several emergent characteristics of empirical roe deer trajectories (Figs 5 and 6). This provides  
242 confidence that the model's realistic predictions of space-use are arising because the model  
243 closely approximates the key characteristics of individual movement behaviour that underlie the  
244 formation of the home ranges.

245         Patterns of animal space-use recorded by GPS-telemetry can be viewed as resulting from  
246 a sequence of movement decisions by the animal about how far to move, and in which direction  
247 i.e., sequences of movement distances and turning angles<sup>9,36</sup>. Our memory-based model was able  
248 to accurately characterize the distributions of both these quantities (Fig. 5). We found that a  
249 realistic, heavy-tailed distribution of step lengths emerged from the combination of a large,  
250 exponentially-weighted motion capacity (that accounts for rare, long steps), and memory-based  
251 attraction (that accounts for the high density of short steps). It has been suggested that  
252 characterizing step lengths with heavy-tailed Gamma or Weibull distributions could improve the  
253 predictive performance of empirically-parametrized movement models<sup>20</sup>. Here we show that  
254 accounting for memory makes this unnecessary. Furthermore, incorporating the effects of  
255 memory also gave rise to frequent reversals in movement directions (i.e., sharp turning angles)  
256 that closely matched the movement behaviour of released roe deer, even though the underlying  
257 redistribution kernel did not include any form of autocorrelation in movement directions.

258         Similarly, home ranges are thought to emerge from the revisitation of specific geographic  
259 locations (also referred to as movement recursions<sup>29</sup>), considered to be the visible manifestations

260 of the influence of memory on movements<sup>11,29</sup>. Our results are consistent with this interpretation.  
261 The resource-only model led to very few revisits, while a revisitation behaviour similar to that  
262 observed in reintroduced roe deer emerged from the memory-based movement simulations (Fig.  
263 6). The memory-based model predicted well the overall distribution of time since last visits,  
264 although it tended to underestimate both short (a day or less) and very long time since last visits  
265 (especially above 100 days) i.e., smaller variance than the observed pattern. The high density of  
266 short-term revisits in observed roe deer trajectories could be the result of daily, local movements  
267 such as an alternation between a foraging ground and a neighbouring area used for shelter<sup>37</sup>. The  
268 discrepancy observed for long-term revisits could instead be due to an artefact of the data  
269 collection (time since last visit can be overestimated in empirical data if visits occur between two  
270 successive GPS relocations), or could reflect biological factors that are not characterized in the  
271 model formulation (e.g., particular environmental conditions may be exploited through proximal  
272 mechanisms such as perception; see Avgar *et al.*<sup>20</sup> for a cognitive model including perception and  
273 memory).

274  
275         Similar to previous studies<sup>15-17</sup>, we hypothesized that home ranges emerge from the  
276 influence of a bi-component memory process in which reference memory captures the long-term  
277 attraction to previously-visited locations, while working memory accounts for a short-term  
278 repulsion (e.g., to adjust to resource dynamics). However, we found that it was not necessary to  
279 include a bi-component memory to give rise to home ranges. This result contrasts with the patch-  
280 to-patch transition model of Van Moorter *et al.*<sup>15</sup>, where absence of working memory leads to  
281 repeated utilization of a sole resource patch. In the memory-based movement formulation used  
282 here, an intrinsic component of resource preference ensures that all locations, including those that

283 have not been visited, or that have been forgotten (i.e., whose reference memory is zero), have a  
284 non-zero probability of being visited at each time step.

285         When fitting the movement model to empirical data, reference memory was the most  
286 influential driver of roe deer movement (Table 1). The learning associated to the initial visit of  
287 any given location led to a 31.6-fold increase in its attraction (Fig. 2a), and hence to a substantial  
288 increase in its probability of being revisited in the future. We found that the influence of memory  
289 on movements was very strong despite the learning rate of reference memory being low.

290 Although, learning was modelled as an exponentially saturating function of experience<sup>38,39</sup>, the  
291 low value of learning rate effectively meant that learning never approached its asymptote, and  
292 was essentially a quasi-linear function of number of visits. In this aspect, our findings provide  
293 support for the simple memory enhanced random walk formulation proposed by Tan *et al.*<sup>40</sup>.  
294 However, in contrast to Tan *et al.*<sup>40</sup>, our formulation also includes a spatial scale of learning  
295 parameter, which was strongly supported (Table 1), and implies that roe deer are likely to return  
296 not only to their previously visited locations but also to adjacent areas (Fig 2a).

297         Reference memory decayed relatively rapidly (half-life of 9.5 days) with time since last  
298 visit. This estimate is relatively consistent with the decay rate reported in a recent experimental  
299 study of roe deer foraging behaviour (half-life of 3.4 days)<sup>21</sup>, but contrasts markedly with the  
300 negligible decay of spatial memory over several months reported for bison (*Bison bison*)<sup>19</sup> and  
301 woodland caribou (*Rangifer tarandus caribou*)<sup>20</sup>. Comparative studies may shed light on whether  
302 the factors underlying the differences in estimated memory decay rates are biological (e.g.,  
303 variation in revisitation patterns linked to differences in movement rates and home range sizes),  
304 or methodological (e.g., between-model differences in the formulations of the cognitive  
305 processes).

306 Our results were, in contrast, much less sensitive to working memory. Working memory  
307 primarily influenced the duration that roe deer spent at visited locations (i.e., residence time).  
308 Because of its nearly instantaneous decay, the repulsion effect of working memory ceased as  
309 soon as the individual left a visited location. As a result, working memory did not influence the  
310 timing of revisits, which contrasts with predictions derived from theoretical movement  
311 simulations<sup>15-17</sup>. The probability that roe deer returned to previously visited locations decreased  
312 monotonically with time since their last visit (Fig. 5d), suggesting that a single memory  
313 component (reference memory, in our case) could capture roe deer revisitation patterns.  
314 Altogether, our results did not support the existence of characteristic multi-day revisitation  
315 periodicities, which would be expected if roe deer relied on working memory to optimally adjust  
316 their visits to underlying resource renewal dynamics. Because roe deer are very selective  
317 browsers, able to switch feeding between an important diversity of plant species<sup>41,42</sup>, it is indeed  
318 unlikely that their foraging behaviour is influenced by short-term dynamics of resource renewal.  
319 In contrast, a bi-component memory process may be more suited to model the foraging behaviour  
320 of species whose resources are concentrated within distinct, continuously-renewing patches such  
321 as grazing lawns in bison<sup>43</sup> or geese<sup>44</sup>.

322  
323 In our study, the estimated memory parameters gave rise to a strong attraction to familiar  
324 locations, consistent with published literature in roe deer<sup>21,28</sup>, and other ungulates<sup>19,45</sup>. Two main  
325 hypotheses have been formulated for the fitness benefits associated with site familiarity: (i)  
326 improved resource acquisition through the memorization of resource locations and attributes<sup>10,15</sup>,  
327 and (ii) predator avoidance through the knowledge of fine-scale variations in predation risk and  
328 of escape routes<sup>46</sup>. Previous work has shown that in roe deer, individuals rely on memory to  
329 efficiently track the spatio-temporal changes in food availability within their familiar

330 environment<sup>21</sup> but are also prone to elevated predation risk from Eurasian lynx (*Lynx lynx*) when  
331 outside of their familiar space<sup>47</sup>. These two benefits of site familiarity are difficult to disentangle  
332 in nature; in our study, both factors may likely have driven the revisitation patterns that  
333 contributed to the emergence of roe deer home ranges.

334 Our analysis also revealed the resource preferences of roe deer in our study area. First, roe  
335 deer exhibited strong preference for intermediate slope steepness (Fig. 2b). Their avoidance of  
336 flat areas is likely explained by the fact that, in the rugged landscape of Aspromonte National  
337 Park, anthropogenic disturbances such as roads and logging activities<sup>48</sup> were concentrated along  
338 valley bottoms, as well as high plateaus. In other ecological systems, these topographic features  
339 have also been associated with elevated predation risk from wolves<sup>49</sup>. Their avoidance of steep  
340 slopes is consistent with roe deer natural history (long limbs, and short and narrow hoofs not  
341 adapted to climbing), and its unsuitability supported by the occurrence of two mortality cases  
342 linked to falls during the reintroduction project (*S. Nicoloso pers. comm.*). Second, roe deer  
343 preferred areas of intermediate-to-high tree cover (Fig. 2c), a finding that is consistent with  
344 published literature on roe deer resource selection<sup>50-52</sup>. Intermediate cover values may indicate  
345 heterogenous environments rich in ecotones, which provide abundant browsing resources<sup>53</sup>.  
346 Third, we found that roe deer strongly preferred reforested areas with young deciduous trees (Fig.  
347 2d), which is likely because these areas provide both cover and abundant browse<sup>42</sup>. Fourth, roe  
348 deer avoided agricultural areas (and associated pastures and settlements; Fig. 2d) in agreement  
349 with existing literature<sup>50,51</sup>.

350 Despite qualitative similarities between the resource-only and memory-based model  
351 formulations, the effect sizes of resource preference parameters were consistently smaller for the  
352 memory-based model than for the resource-only model (Fig. 1; Fig. 2b-d). In absence of memory,  
353 the relative attraction (and hence probability of use) of equally-distant locations solely depends

354 on their respective resource attributes. In contrast, when memory processes operate the relative  
355 attraction is partitioned between two interacting components: resource attributes (i.e., resource  
356 effect), and memory (i.e., site familiarity effect) – thereby reducing the influence of resources *per*  
357 *se*. Because animal home ranges ultimately emerge as the revisitation of familiar, beneficial  
358 resources<sup>10,15</sup>, disentangling the influence of resources from that of site familiarity is challenging  
359 in nature. In particular, where important resource drivers are omitted – either because they are  
360 unknown or because they are not measured – the attraction for familiar areas can be confounded  
361 with attraction for unaccounted resources (i.e., a spurious familiarity effect<sup>54</sup>). Further progress to  
362 characterize the interplay between memory and resource preferences will be contingent on the  
363 ability to identify and quantify underlying spatio-temporal variation in resource patterns. In this  
364 context, combining mechanistic movement models with *in situ* experimental resource  
365 manipulations appears a promising way to disentangle the effects of memory from the effects of  
366 resources<sup>21,28</sup>.

367  
368         Connecting animal movement behaviour to space-use patterns and, ultimately, population  
369 dynamics is a long-term challenge that promises to provide a unifying theory for animal  
370 ecology<sup>55</sup>. In this study, we demonstrated that the interplay between memory and resource  
371 preferences is sufficient to explain the formation of animal home ranges following reintroduction  
372 to a novel environment, and thus contributing to our understanding of the space-use implications  
373 of movement behaviour. The approach utilised here could be expanded to model the  
374 interconnections between movement behaviour and energy acquisition and consumption<sup>56</sup>,  
375 providing a framework to quantitatively characterize the fitness, and demographic consequences  
376 of animal movement patterns, and space-use<sup>57</sup>.

377



378 **Methods**

379 *Roe deer reintroduction*

380 After being extirpated in most of its southern distribution range during the 19<sup>th</sup> century, a roe deer  
381 reintroduction project was undertaken by the Aspromonte National Park (AspNP; Calabria, Italy;  
382 Supplementary S2: Fig. S1) between 2008 and 2011. Ninety-two roe deer were captured in  
383 Sienna County (Tuscany, Italy), of which seventy-five were hard-released at four sites in the  
384 south-west portion of the AspNP (47 females and 28 males). The remaining seventeen either died  
385 during translocation or were not genotyped as *Capreolus capreolus italicus*, the roe deer  
386 subspecies native to the Italian peninsula.

387 The AspNP is 640 sq.km and is characterized by the rugged Aspromonte mountain range  
388 peaking at 1955 m a.s.l, and alternating gorges and torrent river valleys. The climate is  
389 Mediterranean with precipitations concentrated in winter, leading to irregular snow cover above  
390 1000 m a.s.l, and dry and warm summers (annual precipitation: 826 mm; temperature: -0.8/5.4°C  
391 in January, 14.9/23.0°C in August; Gambarie, 1300 m a.s.l). The significant topography within  
392 the region gives rise to a diverse vegetation cover<sup>58</sup> ranging from temperate mountain forests  
393 (e.g., European beech *Fagus sylvatica*, silver fir *Abies alba* and alder *Alnus sp.*) to dry pine and  
394 oak forests (e.g., Calabrese black pine *Pinus laricio*, Mediterranean oaks *Quercus ilex* and  
395 *Quercus suber*), and high Mediterranean maquis (e.g., strawberry tree *Arbutus unedo*, heather  
396 *Erica arborea* and myrtle thickets *Myrto-Pistacietum lentisci*). The region also includes small-  
397 scale, mixed agriculture, orchards and plantations (e.g., chestnut *Castanea sativa*, and olive  
398 groves), pastures at high elevation, as well as small settlements at the margins of the park. Wild  
399 boar (*Sus scrofa*) is the dominant wild ungulate in the study area (red deer, *Cervus elaphus* are  
400 locally extinct). Wolves (*Canis lupus*) are the only natural predators of adult roe deer, although  
401 red fox (*Vulpes vulpes*) may predate upon fawns. Hunting is forbidden within the national park.

402

403 *Empirical data*

404 The movements of twenty-seven individual roe deer were monitored after their release via  
405 telemetry. Roe deer were fitted with GPS-GSM collars scheduled to acquire one relocation every  
406 30 min during the first month after release, and at six-hour intervals thereafter (schedule: 00:00,  
407 06:00, 12:00, 18:00 UTC). For the purpose of our analysis, we retained all animals for which we  
408 could obtain a trajectory of at least 30 days with a high acquisition success rate ( $> 85\%$ ). This  
409 choice led to the exclusion of ten individuals – seven died in the first month after release and  
410 three had malfunctioning collars. Our final sample consisted of 17 roe deer (15 adults: 11  
411 females, 4 males; 2 subadult males), tracked for an average of 281.82 days ( $\sigma = 167.37$ ,  
412 minimum = 39, maximum = 624; Supplementary S3: Table S1).

413 We regularized the trajectories to a homogeneous relocation interval of six hour and did  
414 not interpolate the missing relocations. The final dataset consisted of 19,186 GPS relocations  
415 (acquisition success rate = 93.61%). Roe deer step length averaged 140.04 m between two  
416 successive relocations ( $\sigma = 267.37$ , maximum = 6254.68 m).

417

418 We analysed the movement behaviour of the reintroduced roe deer within a rectangular  
419 area (40.8 x 30 km; 1,224 sq.km; Supplementary S2: Fig. S1), that encompassed all available roe  
420 deer GPS locations and a buffer of 7 km (more than the longest observed step length). Given the  
421 average movement distance of the reintroduced roe deer, and the high landscape heterogeneity of  
422 our study area, the landscape was represented at a spatial resolution of 25 x 25 m.

423 The resource preference component of the mechanistic movement model included both  
424 topographic (slope) and landcover variables (tree cover, agriculture and reforested landcover).  
425 We selected these variables a priori as they are known predictors of roe deer movement and

426 resource selection<sup>42,48,51,52</sup>, and a preliminary step selection analysis (SSA<sup>59</sup>; results not shown)  
427 ascertained their relevance in our study system.

428 We obtained the slope layer from the European Union Digital Elevation Model EU-DEM  
429 v1.0<sup>60</sup>. Slope ranges from 0 to 90°, and was available at a 25 m spatial resolution. We obtained an  
430 estimate of tree cover from Copernicus pan-European, high-resolution layers<sup>61</sup>, 2012 reference  
431 year. Tree cover ranges from 0 to 100%, and was resampled at 25 m from a native spatial  
432 resolution of 20 m. Following preliminary SSA explorations, we (1) calculated tree cover at a  
433 grain of 325 m (i.e., each squared cell of 25 m averaged tree cover within a larger 325 x 325 m  
434 area) and (2) included in the model both linear and quadratic terms for slope and tree cover.

435 Two landcover data sources were available for our study area – a botanical map of high  
436 biological detail and fine spatial resolution (94 categories; 0.05 ha mapping unit) for the  
437 Aspromonte National Park<sup>58</sup>, and the coarser CORINE landcover classification (45 categories; 25  
438 ha mapping unit) for the entire study area<sup>62</sup>, 2012 reference year. Preliminary SSA conducted  
439 within the park boundaries suggested that roe deer selected for areas reforested with deciduous  
440 trees (*Alnus cordata*, *Juglans regia* and *Prunus avium*; hereafter referenced to as *Reforested*), and  
441 avoided spatially-dominant agriculture areas (olive groves, cultivated fields, mixed agriculture),  
442 and more localized pastures and anthropized areas (hereafter referenced to as *Agriculture*).  
443 Outside the park, we assumed that there were no *Reforested* areas, and used CORINE to map  
444 *Agriculture* – choices that we validated by visually inspecting the satellite images in the vicinity  
445 (< 1 km) of the roe deer relocations outside of the park.

446  
447 *Modelling approach*

448 We modelled the movement of reintroduced roe deer using an individual-based, spatially explicit  
449 *redistribution kernel* combining spatial memory and resource preferences. Specifically, we

450 defined the probability of moving between the relocation  $\mathbf{x}_{t-1}$  and the relocation  $\mathbf{x}_t$  (as it is  
451 standard:  $\mathbf{x} = (x, y)$ ), as the normalized product of an *information-independent movement*  
452 *kernel*<sup>27</sup>,  $k(\mathbf{x}_t; \mathbf{x}_{t-1}, \theta_1)$ , and a *cognitive weighting function*,  $w(\mathbf{x}_t; t, \theta_2)$ <sup>20,26</sup>:

$$453 \quad p(\mathbf{x}_t | \mathbf{x}_{t-1}, \theta_1, \theta_2) = \underbrace{k(\mathbf{x}_t; \mathbf{x}_{t-1}, \theta_1)}_{\text{Movement kernel}} \cdot \underbrace{w(\mathbf{x}_t; t, \theta_2)}_{\text{Weighting function}} \cdot \underbrace{\left[ \sum_{\mathbf{u} \in \Omega} k(\mathbf{u}; \mathbf{x}_{t-1}, \theta_1) \cdot w(\mathbf{u}; t, \theta_2) \right]^{-1}}_{\text{Normalization over spatial domain } \Omega} \quad \text{Eq. 1}$$

454  
455 with  $\mathbf{u} = (x, y)$  denoting all the locations within the within the spatial domain  $\Omega$ , and  $\theta_1$  and  $\theta_2$   
456 the ensemble of parameters governing the movement kernel, and the weighting function,  
457 respectively.

458  
459 *Motion capacity – the information-independent movement kernel*  
460 The information-independent movement kernel characterizes the movement of an animal  
461 independently of its cognitive abilities and of the surrounding landscape, and therefore quantifies  
462 its motion capacity<sup>20</sup>. It is obtained through the product of two probability distributions: step  
463 length,  $S$ , and movement direction,  $\Phi$ . Here, we modelled roe deer step length using a truncated  
464 Weibull distribution. The Weibull distribution is governed by two parameters – the shape ( $\kappa_S >$   
465 0) and the rate ( $\lambda_S \geq 0$ ), and can account for both a high density of short movements and rare,  
466 long movements (i.e., heavy tail), typical of empirical data of animal movement<sup>63</sup>. To reduce the  
467 computational power required for model fitting, we assumed that roe deer movement probability  
468 was zero beyond 7 km (maximum observed step length = 6.25 km). The resulting step length  
469 distribution for any location  $\mathbf{u}$  is given by:

470  $S(\|\mathbf{u} - \mathbf{x}_{t-1}\|; \kappa_S, \lambda_S)$   
471  $= \begin{cases} \lambda_S \kappa_S (\lambda_S \|\mathbf{u} - \mathbf{x}_{t-1}\|)^{\kappa_S - 1} e^{-(\lambda_S \|\mathbf{u} - \mathbf{x}_{t-1}\|)^{\kappa_S}}, & \|\mathbf{u} - \mathbf{x}_{t-1}\| \leq 7 \text{ km} \\ 0, & \text{otherwise} \end{cases} \quad \text{Eq. 2}$

472

473 We modelled roe deer movement directions as a circular normal distribution such that:

474  $\Phi = \frac{1}{2\pi} \quad \text{Eq. 3}$

475

476 It follows that the information-independent movement kernel is given by:

477  $k(\mathbf{u}; \mathbf{x}_{t-1}, \kappa_S, \lambda_S) = \frac{S(\|\mathbf{u} - \mathbf{x}_{t-1}\|; \kappa_S, \lambda_S) \Phi}{\|\mathbf{u} - \mathbf{x}_{t-1}\|} \quad \text{Eq. 4}$

478

479 where the denominator  $\|\mathbf{u} - \mathbf{x}_{t-1}\|$  translates polar coordinates into Euclidean coordinates i.e.,

480 the conversion of a probability of moving a given distance and direction to a probability of

481 moving to a particular area<sup>9</sup>. Given the temporal resolution of our movement data (every 6 h), we

482 ignored serial correlation in movement direction. Because we fitted our mechanistic movement

483 model to observed movement data in a discretized landscape (square cells of resolution 25 m), we

484 transformed the GPS relocations in the continuous space,  $\mathbf{x}_t$ , to the centroid of the overlapping

485 cell (see Supplementary S4 for the correction required to calculate the movement kernel on the

486 location currently used by the animal).

487

488 *Interplay between memory and resource preferences – the cognitive weighting function*

489 The interaction between the landscape and the animal cognitive abilities was represented via the

490 weighting function  $w$ . We assumed that animal movement was influenced by memory,  $m(\mathbf{u}; t)$ ,

491 and that, in absence of such information, animals may visit locations in proportion to their  
492 intrinsic resource preference value:

$$493 \quad w(\mathbf{u}; t, \varepsilon) = \left[ \begin{array}{c} \underbrace{m(\mathbf{u}; t)}_{\text{Memory}} + \underbrace{\varepsilon}_{\text{Intrinsic}} \\ \text{component} \quad \text{component} \end{array} \right] \underbrace{Q(\mathbf{u})}_{\text{Resource}} \quad \text{Eq. 5} \\ \text{preference}$$

494  
495 with  $\varepsilon$ , the intrinsic component of resource preference. In our model formulation, it is not the  
496 absolute value of memory that defines its influence on movement, but rather its value relative to  
497 the intrinsic component of resource preference i.e., scaled to the attraction of similar resource  
498 conditions in absence of memory. We modelled the preference for location  $\mathbf{u}$ ,  $Q(\mathbf{u})$ , using an  
499 exponential resource selection<sup>64</sup>:

$$500 \quad Q(\mathbf{u}) = e^{(\beta_1 \text{slope} + \beta_2 \text{slope}^2 + \beta_3 \text{cover} + \beta_4 \text{cover}^2 + \beta_5 LC_{\text{reforested}} + \beta_6 LC_{\text{agriculture}})} \quad \text{Eq. 6}$$

501  
502 with  $\beta_i$  the selection coefficient for resource variable  $i$  – slope (linear and quadratic terms), tree  
503 cover (linear and quadratic terms), and reforested and agriculture landcovers – evaluated at  
504 location  $\mathbf{u}$ .

505 We modelled memory,  $m(\mathbf{u}; t)$ , as a bi-component mechanism<sup>15–17</sup>. Reference memory,  
506  $m_R(\mathbf{u}; t)$ , is the long-term memory of previously-visited spatial locations and has an attractive  
507 effect. By contrast, the working memory,  $m_W(\mathbf{u}; t)$ , encodes the short-term, temporary repulsion  
508 of previously visited locations. The combined memory map is given by:

$$509 \quad m(\mathbf{u}; t) = m_R(\mathbf{u}; t) - m_W(\mathbf{u}; t) \quad \text{Eq. 7}$$

510  
511 The dynamics of both memory components are governed by learning (i.e., acquisition of  
512 information) and decay or forgetting (i.e., loss of information). The learning curve was

513 represented by an asymptotically increasing function of experience<sup>38,39</sup>. Specifically, we  
 514 formulated learning as an exponentially saturating process with an associated spatial scale such  
 515 that animals experience maximum learning at their current position, but also gain information  
 516 about surrounding areas. Decay was modelled as a negative exponential of time since last  
 517 visit<sup>65,66</sup>. Together this yields the following equations for the dynamics of memory across space  
 518  $\mathbf{u}$ , given the animal's current position  $\mathbf{x}_t$ :

$$519 \quad m_j(\mathbf{u}; t, \mathbf{x}_{t-1}) = m_j(\mathbf{u}; t - 1) + \underbrace{\alpha(\mathbf{u}; \mathbf{x}_{t-1}, \lambda_j) \cdot (1 - m_j(\mathbf{u}; t - 1))}_{\text{Learning}} \cdot l_j$$

$$520 \quad - \underbrace{(1 - \alpha(\mathbf{u}; \mathbf{x}_{t-1}, \lambda_j)) \cdot m_j(\mathbf{u}; t - 1)}_{\text{Decay}} \cdot \delta_j \quad \text{Eq. 8}$$

521

$$522 \quad \alpha(\mathbf{u}; \mathbf{x}_{t-1}, \lambda_j) = e^{-\lambda_j \cdot \|\mathbf{u} - \mathbf{x}_{t-1}\|} \quad \text{Eq. 9}$$

523

524 where  $J = R$  and  $J = W$  for reference and working memory, respectively;  $l_R$  and  $l_W$  are the rates  
 525 of learning for reference and working memory; the functions  $\alpha(\mathbf{u}; \mathbf{x}_{t-1}, \lambda_R)$  and  $\alpha(\mathbf{u}; \mathbf{x}_{t-1}, \lambda_W)$   
 526 respectively describe how the rates of reference and working memory acquisition attenuate as a  
 527 function of distance from the animal's previous position (modelled via negative exponential  
 528 functions); and  $\delta_R$  and  $\delta_W$  determine the rates at which the two forms of memory decay over  
 529 time. According to their biological definition<sup>15,16</sup>, reference memory is always larger than  
 530 working memory, thus imposing the following constraints:  $l_R \geq l_W$ ,  $\delta_R \leq \delta_W$  and  $\lambda_R \leq \lambda_W$ . For  
 531 missing relocations, no learning occurred but memory decay took place.

532

533 *Model fitting*

534 We fitted two models representing competing hypotheses pertaining to the biological processes  
535 influencing the movements of reintroduced roe deer: resource-only ( $M_{\text{res}}$ ), and interplay between  
536 memory and resources ( $M_{\text{mem:res}}$ ). For the  $M_{\text{res}}$  model, the memory parameters were omitted (i.e.,  
537 no memory learning;  $l_R = l_W = 0$ ). We estimated the model parameters through maximum-  
538 likelihood inference. The likelihood function for the parameter set of the information-  
539 independent movement kernel  $\theta_1 = \kappa_S, \lambda_S$ , and of the cognitive weighting function,  $\theta_2 =$   
540  $(l_R, l_W, \delta_R, \delta_W, \lambda_R, \lambda_W, \varepsilon, \beta_1: \beta_6)$ , is given as:

$$541 \quad L(\boldsymbol{\omega}) = \prod_{i=1}^N \prod_{t=1}^{T_i} p(\mathbf{x}_t | \mathbf{x}_{t-1}, \theta_1, \theta_2) \quad \text{Eq. 10}$$

542  
543 with  $N$  the number of animals (i.e., 17) and  $T_i$  the number of relocations for animal  $i$ . Missing  
544 GPS relocations were omitted from the likelihood function. We estimated the global minima of  
545 the log-likelihood function [ $\log L(\boldsymbol{\omega})$ ; i.e., the objective function] using the particle swarm  
546 optimization algorithm (PSO<sup>67</sup>; see Supplementary S5 for details). We calculated 95% marginal  
547 confidence intervals (CIs) via an asymptotic normal approximation of the objective function in  
548 the neighbourhood of the global minima. We then evaluated the contribution of each variable to  
549 the model support by calculating the delta Akaike Information Criterion<sup>68</sup> of the reduced model  
550 (i.e., excluding the variable of interest) relative to the full model.

551

### 552 *Movement simulations and emergent properties*

553 We evaluated whether the two parametrized movement models ( $M_{\text{res}}$  and  $M_{\text{mem:res}}$ ) could  
554 characterize the spatial behaviour of reintroduced roe deer by means of movement simulations.  
555 For each monitored roe deer, we ran 30 movement simulations (17 animals x 30 runs = 510



556 simulated trajectories per model), initiated on the first observed GPS relocation of each  
557 individual (i.e., in the vicinity of the release site). At each time step, a spatial location was  
558 randomly selected according to the probabilities defined by the parametrized redistribution  
559 kernel. Simulations ran for a duration equivalent to that of the observed roe deer trajectories.

560 We compared observed and simulated trajectories using key emerging properties. First, to  
561 evaluate the emergence of spatially-restricted movements, we compared the temporal trend in net  
562 squared displacement (NSD). NSD was calculated as the squared distance between the individual  
563 position at time  $t$ ,  $\mathbf{x}_t$ , and the trajectory start position,  $\mathbf{x}_0$ :

$$564 \quad \quad \quad NSD_t = \|\mathbf{x}_t - \mathbf{x}_0\|^2 \quad Eq. 11$$

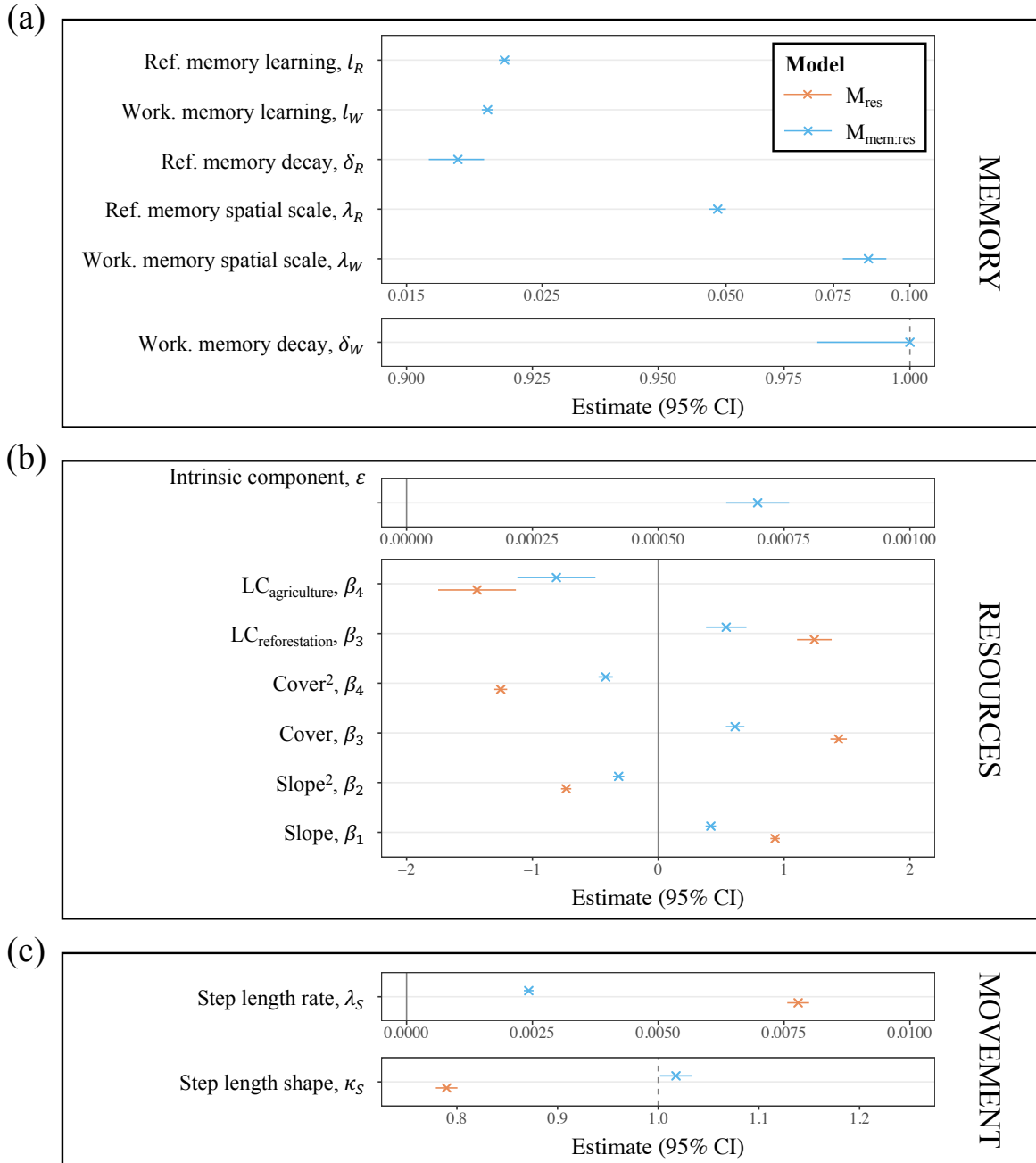
565  
566 At the population-level, we computed the mean NSD for the 17 released roe deer as a 5-day  
567 running mean to remove individual noise. For the simulations, we calculated the 5% and 95%  
568 confidence bounds for the mean NSD via bootstrapping (1000 random samples of 17 simulated  
569 trajectories). Second, we evaluated whether the parametrized movement models captured the  
570 empirical distributions of emergent movement properties. We calculated step length as the  
571 Euclidean distance between two successive relocations, and turning angle as the angle in radians  
572 between the directions of two successive steps (ranges from  $-\pi$  to  $\pi$ ; 0 indicating no directional  
573 change). Third, we investigated whether the parametrized movement models captured roe deer  
574 revisitation behaviour (i.e., movement recursions<sup>29</sup>). Revisits, defined as returns to a previously  
575 visited area, occurred when an animal (observed or simulated) used a 25 x 25 m spatial cell that  
576 had been last visited within  $> 6$  hours (i.e., temporally-disjointed use of a specific location). For  
577 each visited cell along the trajectory, we computed its total number of revisits (0 indicating a  
578 single visit) and their associated time since last visit.

579  
580           Equations 1-10 were solved numerically, and simulations performed in C++. The  
581 parameters were estimated using the PSO algorithm, implemented within the Global  
582 Optimization Toolbox, MATLAB R2017b (MathWorks, Natick, Massachusetts, USA). The  
583 optimization ran on a computer cluster using the Distributed Computer Server<sup>69</sup>. We calculated  
584 the CIs, produced the effect size plots and comparison between observed and simulated  
585 trajectories in R<sup>70</sup>.

586 **Table 1 Variable contributions to the memory-based model ( $M_{\text{mem:res}}$ ).**

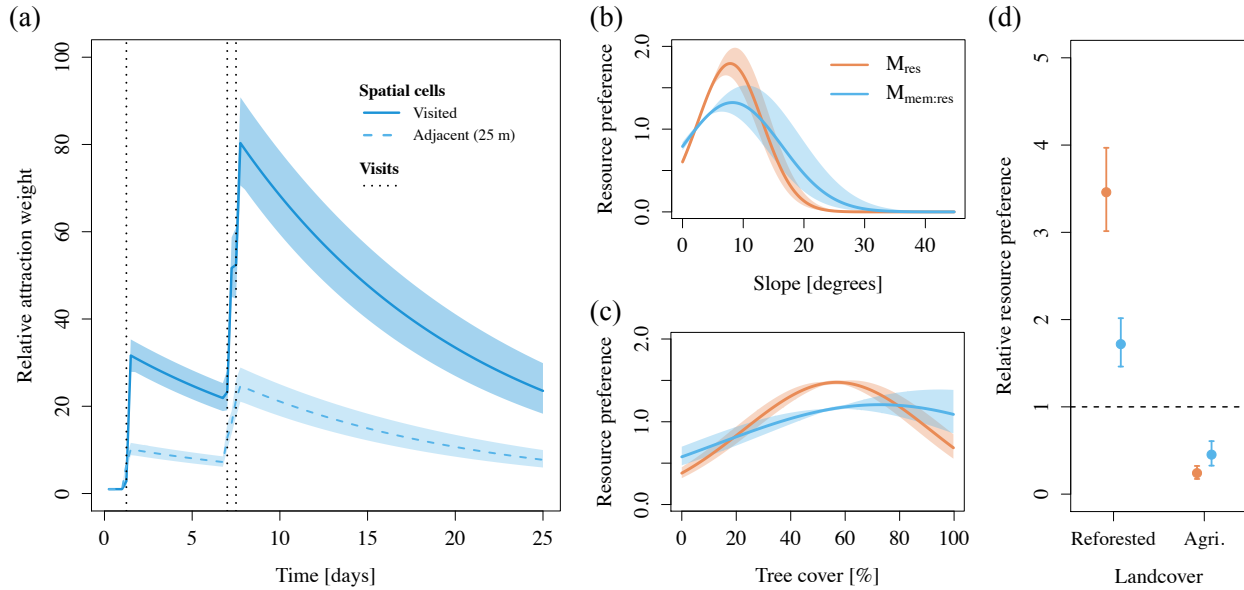
Variable(s) removed from		Number of removed		
the full model	Equation(s)	Parameter setting(s)	parameters	$\Delta$ AIC
Ref. memory (i.e., $M_{\text{res}}$ )	7, 8	$l_R = 0^*$	6	17,355
Ref. memory spatial scale	8, 10	$\lambda_R = \infty$	1	7,444
Step length decay	2	$\lambda_S = 0$	1	4,945
Ref. memory learning	8	$l_R = 1$	1	3,434
Ref. memory decay	8	$\delta_R = 0$	1	2,631
Working memory	7, 9	$l_W = 0^{**}$	3	1,278
All resources	6	$\beta_1 : \beta_6 = 0$	6	304
Slope + Slope <sup>2</sup>	6	$\beta_1 = \beta_2 = 0$	2	138
Landcover – reforested	6	$\beta_6 = 0$	1	83
Landcover – agriculture	6	$\beta_5 = 0$	1	59
Cover + Cover <sup>2</sup>	6	$\beta_3 = \beta_4 = 0$	2	34
Step length rate	2	$\kappa_S = 1$	1	4

587 Variable importance is calculated as the delta AIC of the reduced model (i.e., excluding the variable of  
588 interest) relative to the full model. Equations refer to the numbered formulations in the *Methods* section.  
589 Parameters setting refers to the conditions imposed to exclude the variable. \*Reference (Ref.) memory was  
590 removed by setting its learning rate,  $l_R = 0$ , resulting in the effective removal of all memory parameters (i.e.,  
591 equivalent to a resource-only model):  $\lambda_R$  and  $\delta_R$  are irrelevant if there is no reference memory learning, and  
592 because  $l_W \leq l_R$ , the three working memory parameters ( $l_W$ ,  $\lambda_W$  and  $\delta_W$ ) were dropped as well. \*\*Similarly,  
593 removing working memory by setting  $l_R = 0$ , led to the effective removal of  $\lambda_W$  and  $\delta_W$ .  
594

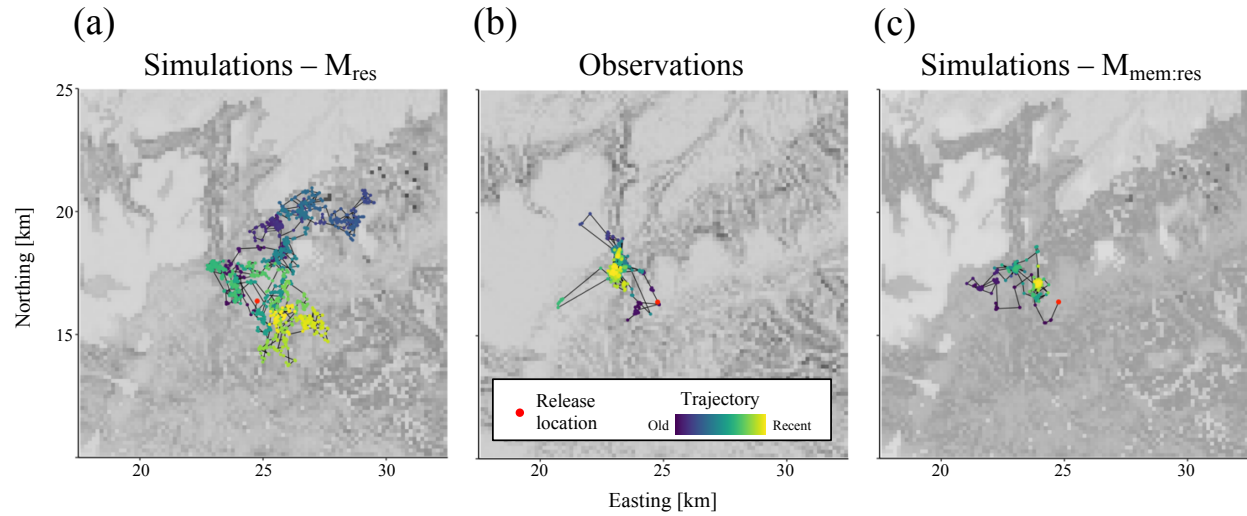


595

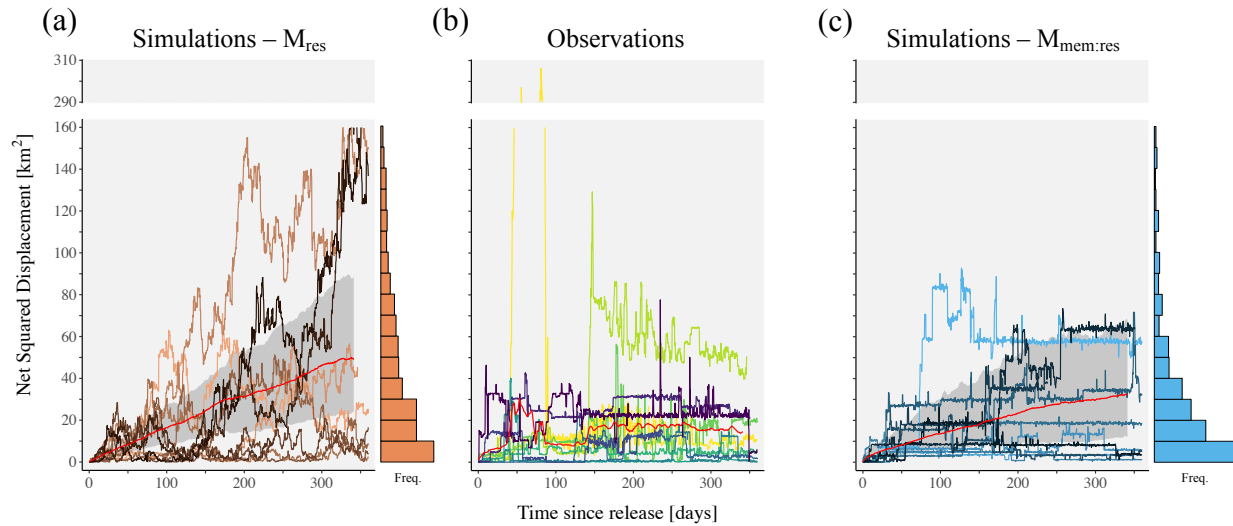
596 **Figure 1: Parameter estimates.** The estimates for the resource-only ( $M_{res}$ ; orange), and the memory-based  
 597 ( $M_{mem.res}$ ; blue) models are plotted with the corresponding 95% marginal confidence intervals. Memory  
 598 (panel a), resource preference (b) and movement (c) parameters are shown separately for readability.



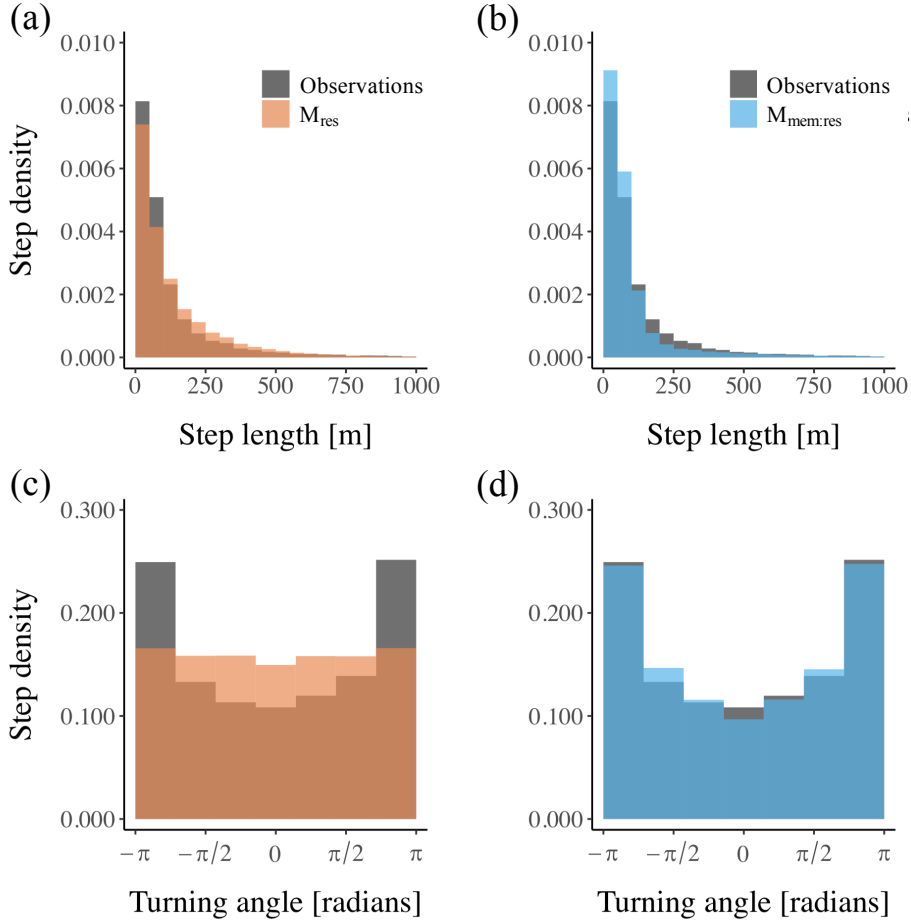
599  
600 **Figure 2: Predictor effects.** The response curves for the resource-only ( $M_{res}$ ; orange) and the memory-  
601 based ( $M_{mem:res}$ ; blue) models are plotted with the corresponding 95% marginal confidence intervals. Panel  
602 (a) shows the attraction of a visited spatial cell (continuous line) and an adjacent cell (25 m away; dashed  
603 line) relative to a cell that has never been visited (attraction = 1) resulting from the fitted memory-based  
604 model. Hypothetical visits (at  $t = 1.25, 7.00$  and  $7.50$  days) are shown in dotted vertical lines. Panel (b) and  
605 (c) illustrate the preference for slope and tree cover, respectively. Panel (d) shows the relative preference  
606 for reforested and agriculture landcovers.  
607



608  
609 **Figure 3: Movement trajectories.** Three typical trajectories are shown for the resource-only simulations  
610 ( $M_{res}$ ; panel a), observed roe deer movements (panel b), and memory-based simulations ( $M_{mem.res}$ ; panel c).  
611 The release location is shown as a red dot and the time since release illustrated as a colour gradient (blue  
612 = old, yellow = recent). The trajectories were selected from the sample displayed on Figure 4.  
613

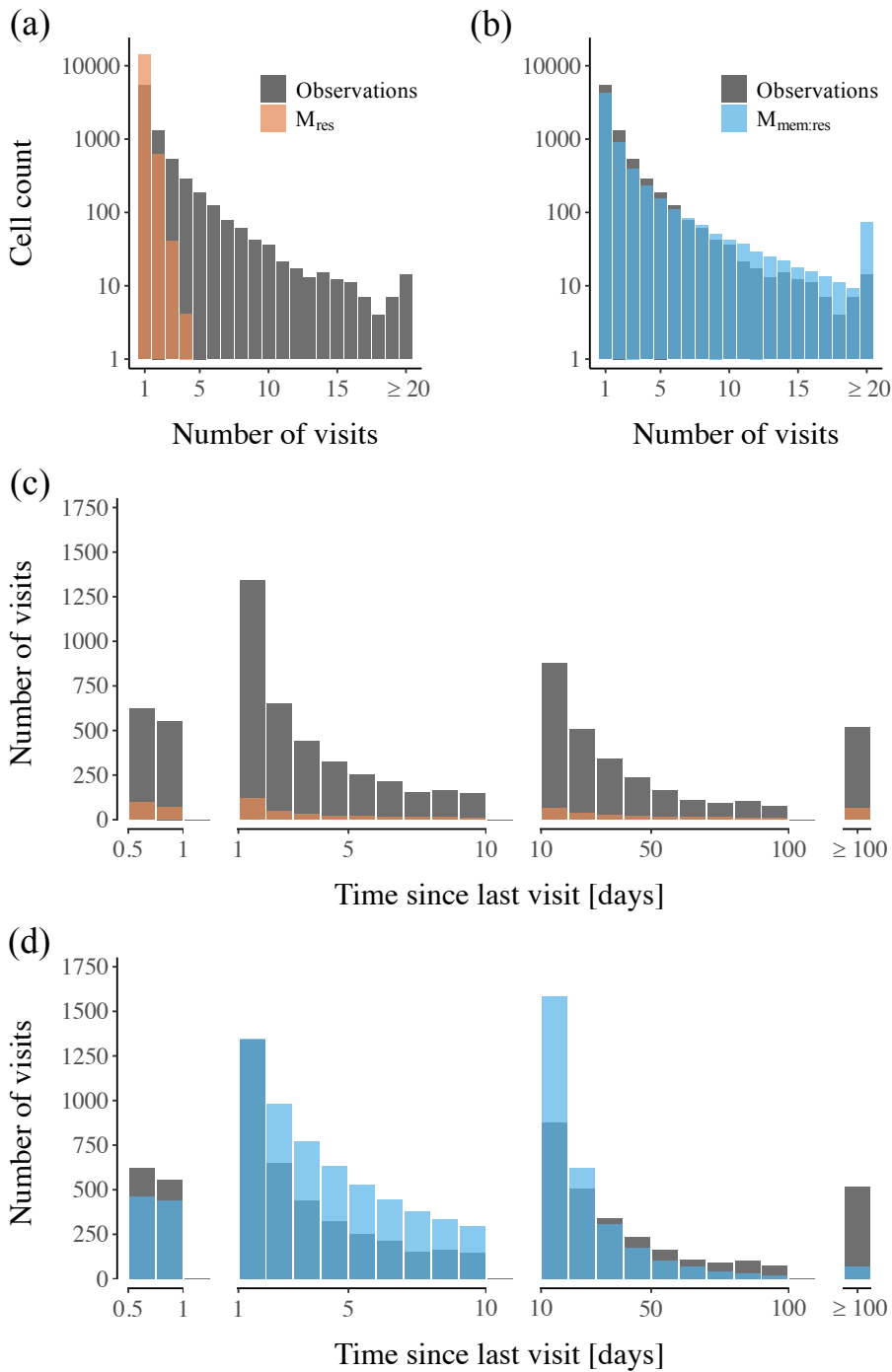


614  
615 **Figure 4: Trends in net squared displacement (NSD) with time since release.** Panel (a): resource-only  
616 simulations ( $M_{res}$ ). Panel (b): observed roe deer movements. Panel (c): memory-based simulations  
617 ( $M_{mem:res}$ ). For the sake of clarity, only the individuals with more than 230 days of monitoring are shown ( $n =$   
618 10). For the simulations, one run for each of the selected individuals was randomly chosen. The trends in  
619 mean NSD across individuals are plotted as solid red lines (grey ribbons indicate the 5% and 95%  
620 bootstrapped quantiles for the simulations; panels a and c). The vertical histograms show the frequency of  
621 final NSD (i.e., evaluated at the end of the trajectories) for the simulations.  
622



623  
624 **Figure 5: Emergent movement properties.** The distributions of step length (panels a and b) and turning  
625 angle (panels c and d) are shown for observed roe deer movements (grey), the simulated trajectories from  
626 the resource-only model ( $M_{res}$ ; orange), and the simulated trajectories from the memory-based model  
627 ( $M_{mem:res}$ ; blue).





628  
 629 **Figure 6: Emergent revisitation properties.** The distributions of revisits (panels a and b) and time since  
 630 last visit (panels c and d) are shown for observed roe deer movements (grey), the simulated trajectories  
 631 from the resource-only model ( $M_{res}$ ; orange), and the simulated trajectories from the memory-based model  
 632 ( $M_{mem:res}$ ; blue).

633 **Acknowledgments**

634 N. Ranc was supported by a Harvard University Graduate Fellowship and a Fondazione  
635 Edmund Mach International Doctoral Programme Fellowship. F. Cagnacci was supported by the  
636 Sarah and Daniel Hrdy Fellowship 2015-2016 at Harvard University OEB during part of the  
637 development of this manuscript. We thank the Aspromonte National Park (Calabria, Italia) for  
638 promoting and financially supporting the roe deer reintroduction project, and the applied ecology  
639 (agriculture, forestry and wildlife management) cooperative *D.R.E.Am. Italia* (Tuscany, Italy).  
640 We especially and warmly thank Sandro Nicoloso and Lillia Orlandi (*D.R.E.Am. Italia*), and  
641 Antonino Morabito (*Legambiente*). We are also very grateful to P. Krastev (Harvard Research  
642 Computing), A. La Fata, B. Ölveczky, N. Pierce and J.W. Cain for their valuable suggestions.

643

644 **Competing Interest Statement**

645 The authors declare no competing interests.

646

647 **Data Availability Statement**

648 The datasets generated and/or analysed during the current study are available from the authors on  
649 request.

650

651 **Ethical Statement**

652 The roe deer (*Capreolus capreolus spp. italicus*) reintroduction project was carried out under the  
653 technical approval and ethical requirements of the Institute for Environmental Protection and  
654 Research (ISPRA, public body for research under the vigilance of the Italian Ministry of the  
655 Environment; protocols #47427 and #45826). The capture of roe deer in the population of origin

656 were conducted under authorization #1555 by the Director of the Wildlife Resources and Natural  
657 Reserve Service of the Province of Sienna.

658

## 659 **References**

660 1. Burt, W. H. Territoriality and home range concepts as applied to mammals. *J. Mammal.*

661 **24**, 346–352 (1943).

662 2. Riotte-Lambert, L., Benhamou, S., Bonenfant, C. & Chamaillé-Jammes, S. Spatial

663 memory shapes density dependence in population dynamics. *Proc. R. Soc. B Biol. Sci.* **284**,

664 20171411 (2017).

665 3. Lewis, M. A. & Murray, J. D. Modelling territoriality and wolf-deer interactions. *Nature*

666 **366**, 738–740 (1993).

667 4. White, P. C. L., Harris, S. & Smith, G. C. Fox contact behaviour and rabies spread: a

668 model for the estimation of contact probabilities between urban foxes at different

669 population densities and its implications for rabies control in Britain. *J. Appl. Ecol.* **32**,

670 693–706 (1995).

671 5. Schofield, G. *et al.* Inter-annual variability in the home range of breeding turtles:

672 implications for current and future conservation management. *Biol. Conserv.* **143**, 722–730

673 (2010).

674 6. Börger, L., Dalziel, B. D. & Fryxell, J. M. Are there general mechanisms of animal home

675 range behaviour? A review and prospects for future. *Ecol. Lett.* **11**, 637–650 (2008).

676 7. Moorcroft, P. R., Lewis, M. A. & Crabtree, R. L. Mechanistic home range models capture

677 spatial patterns and dynamics of coyote territories in Yellowstone. *Proc. R. Soc. B Biol.*

678 *Sci.* **273**, 1651–1659 (2006).

679 8. Bateman, A. W., Lewis, M. A., Gall, G., Manser, M. B. & Clutton-Brock, T. H.

- 680 Territoriality and home-range dynamics in meerkats, *Suricata suricatta*: a mechanistic  
681 modelling approach. *J. Anim. Ecol.* **84**, 260–271 (2015).
- 682 9. Moorcroft, P. R. & Lewis, M. A. *Mechanistic home range analysis*. (Princeton University  
683 Press, 2006).
- 684 10. Spencer, W. D. Home ranges and the value of spatial information. *J. Mammal.* **93**, 929–  
685 947 (2012).
- 686 11. Fagan, W. F. *et al.* Spatial memory and animal movement. *Ecol. Lett.* **16**, 1316–1329  
687 (2013).
- 688 12. Fronhofer, E. A., Hovestadt, T. & Poethke, H. J. From random walks to informed  
689 movement. *Oikos* **122**, 857–866 (2013).
- 690 13. Boyer, D. & Walsh, P. D. Modelling the mobility of living organisms in heterogeneous  
691 landscapes: does memory improve foraging success? *Philos. Trans. R. Soc. A Math. Phys.*  
692 *Eng. Sci.* **368**, 5645–5659 (2010).
- 693 14. Benhamou, S. Spatial memory and searching efficiency. *Animal Behaviour* **47**, 1423–1433  
694 (1994).
- 695 15. Van Moorter, B. *et al.* Memory keeps you at home: a mechanistic model for home range  
696 emergence. *Oikos* **118**, 641–652 (2009).
- 697 16. Bracis, C., Gurarie, E., Van Moorter, B. & Goodwin, R. A. Memory effects on movement  
698 behavior in animal foraging. *PLoS One* **10**, e0136057 (2015).
- 699 17. Riotte-Lambert, L., Benhamou, S. & Chamailé-Jammes, S. How memory-based  
700 movement leads to nonterritorial spatial segregation. *Am. Nat.* **185**, E103–116 (2015).
- 701 18. González-Gómez, P. L., Bozinovic, F. & Vásquez, R. A. Elements of episodic-like  
702 memory in free-living hummingbirds, energetic consequences. *Anim. Behav.* **81**, 1257–  
703 1262 (2011).

- 704 19. Merkle, J. A., Fortin, D. & Morales, J. M. A memory-based foraging tactic reveals an  
705 adaptive mechanism for restricted space use. *Ecol. Lett.* **17**, 924–931 (2014).
- 706 20. Avgar, T. *et al.* Space-use behaviour of woodland caribou based on a cognitive movement  
707 model. *J. Anim. Ecol.* **84**, 1059–1070 (2015).
- 708 21. Ranc, N., Cagnacci, F., Ossi, F. & Moorcroft, P. R. Experimental evidence of memory-  
709 based foraging decisions in a resident large mammal. *bioRxiv* **112912v1**, (2020).
- 710 22. Merkle, J. A., Potts, J. R. & Fortin, D. Energy benefits and emergent space use patterns of  
711 an empirically parameterized model of memory-based patch selection. *Oikos* **126**, 185–196  
712 (2017).
- 713 23. Schlägel, U. E., Merrill, E. H. & Lewis, M. A. Territory surveillance and prey  
714 management: wolves keep track of space and time. *Ecol. Evol.* **7**, 8388–8405 (2017).
- 715 24. Hewison, A. J. M., Vincent, J.-P. & Reby, D. Social organisation of European roe deer. in  
716 *The European roe deer: the biology of success* (eds. Andersen, R., Duncan, P. & Linnell, J.  
717 D. C.) 189–219 (Scandinavian University Press, 1998).
- 718 25. Dall, S. R. X., Giraldeau, L. A., Olsson, O., McNamara, J. M. & Stephens, D. W.  
719 Information and its use by animals in evolutionary ecology. *Trends Ecol. Evol.* **20**, 187–  
720 193 (2005).
- 721 26. Schlägel, U. E. & Lewis, M. A. Detecting effects of spatial memory and dynamic  
722 information on animal movement decisions. *Methods Ecol. Evol.* **5**, 1236–1246 (2014).
- 723 27. Moorcroft, P. R. & Barnett, A. Mechanistic home range models and resource selection  
724 analysis: a reconciliation and unification. *Ecology* **89**, 1112–1119 (2008).
- 725 28. Ranc, N. *et al.* Preference and familiarity mediate spatial responses of a large herbivore to  
726 experimental manipulation of resource availability. *Sci. Rep.* **10**, 11946 (2020).
- 727 29. Berger-Tal, O. & Bar-David, S. Recursive movement patterns: review and synthesis across

- 728 species. *Ecosphere* **6**, 1–12 (2015).
- 729 30. Cagnacci, F., Boitani, L., Powell, R. A. & Boyce, M. S. Animal ecology meets GPS-based  
730 radiotelemetry: A perfect storm of opportunities and challenges. *Philos. Trans. R. Soc. B*  
731 *Biol. Sci.* **365**, 2157–2162 (2010).
- 732 31. Nabe-Nielsen, J., Tougaard, J., Teilmann, J., Lucke, K. & Forchhammer, M. C. How a  
733 simple adaptive foraging strategy can lead to emergent home ranges and increased food  
734 intake. *Oikos* **122**, 1307–1316 (2013).
- 735 32. Potts, J. R. & Lewis, M. A. How do animal territories form and change? Lessons from 20  
736 years of mechanistic modelling. *Proc. R. Soc. B Biol. Sci.* **281**, (2014).
- 737 33. Moorcroft, P. R., Lewis, M. A. & Crabtree, R. L. Home range analysis using a mechanistic  
738 home range model. *Ecology* **80**, 1656–1665 (1999).
- 739 34. Bracis, C. & Mueller, T. Memory, not just perception, plays an important role in terrestrial  
740 mammalian migration. *Proc. R. Soc. B Biol. Sci.* **284**, 20170449 (2017).
- 741 35. Potts, J. R., Mokross, K. & Lewis, M. A. A unifying framework for quantifying the nature  
742 of animal interactions. *J. R. Soc. Interface* **11**, (2014).
- 743 36. Turchin, P. *Quantitative analysis of movement: measuring and modeling population*  
744 *redistribution in animals and plants*. (Sinauer Associates, 1998).
- 745 37. Mysterud, A. & Østbye, E. Bed-site selection by European roe deer (*Capreolus capreolus*)  
746 in southern Norway during winter. *Can. J. Zool.* **73**, 924–932 (1995).
- 747 38. Estes, W. K. Toward a statistical theory of learning. *Psychol. Rev.* **57**, 94–107 (1950).
- 748 39. Bush, R. R. & Mosteller, F. A mathematical model for simple learning. *Psychol. Rev.* **58**,  
749 313–323 (1951).
- 750 40. Tan, Z. J., Zou, X. W., Huang, S. Y., Zhang, W. & Jin, Z. Z. Random walk with memory  
751 enhancement and decay. *Phys. Rev. E - Stat. Physics, Plasmas, Fluids, Relat. Interdiscip.*

- 752 *Top.* **65**, 5 (2002).
- 753 41. Duncan, P., Tixier, H., Hoffman, R. R. & Lechner-Doll, M. Feeding strategies and the  
754 physiology in roe deer. in *The European roe deer: the biology of success* (eds. Andersen,  
755 R., Duncan, P. & Linnell, J. D. C.) 91–116 (Scandinavian University Press, 1998).
- 756 42. Mancinelli, S., Peters, W., Boitani, L., Hebblewhite, M. & Cagnacci, F. Roe deer summer  
757 habitat selection at multiple spatio-temporal scales in an alpine environment. *Hystrix* **26**,  
758 132–140 (2015).
- 759 43. Geremia, C. *et al.* Migrating bison engineer the green wave. *Proc. Natl. Acad. Sci. U. S. A.*  
760 **116**, 25707–25713 (2019).
- 761 44. Person, B. T. *et al.* Feedback dynamics of grazing lawns: coupling vegetation change with  
762 animal growth. *Oecologia* **135**, 583–592 (2003).
- 763 45. Wolf, M., Frair, J., Merrill, E. & Turchin, P. The attraction of the known: the importance  
764 of spatial familiarity in habitat selection in wapiti *Cervus elaphus*. *Ecography (Cop.)*. **32**,  
765 401–410 (2009).
- 766 46. Metzgar, L. H. An experimental comparison of screech owl predation on resident and  
767 transient white-footed mice (*Peromyscus leucopus*). *J. Mammal.* **48**, 387 (1967).
- 768 47. Gehr, B. *et al.* Stay home, stay safe - site familiarity reduces predation risk in a large  
769 herbivore in two contrasting study sites. *J. Anim. Ecol.* **89**, 1329–1339 (2020).
- 770 48. Coulon, A. *et al.* Inferring the effects of landscape structure on roe deer (*Capreolus*  
771 *capreolus*) movements using a step selection function. *Landsc. Ecol.* **23**, 603–614 (2008).
- 772 49. Hebblewhite, M., Merrill, E. H. & McDonald, T. L. Spatial decomposition of predation risk  
773 using resource selection functions: an example in a wolf-elk predator-prey system. *Oikos*  
774 **111**, 101–111 (2005).
- 775 50. Morellet, N. *et al.* Landscape composition influences roe deer habitat selection at both

- 776 home range and landscape scales. *Landsc. Ecol.* **26**, 999–1010 (2011).
- 777 51. Tufto, J., Andersen, R. & Linnell, J. Habitat use and ecological correlates of home range  
778 size in a small cervid: the roe deer. *J. Anim. Ecol.* **65**, 715–724 (1996).
- 779 52. De Groeve, J. *et al.* Individual Movement - Sequence Analysis Method (IM-SAM):  
780 characterizing spatio-temporal patterns of animal habitat use across landscapes. *Int. J.*  
781 *Geogr. Inf. Sci.* **0**, 1–22 (2019).
- 782 53. Saïd, S. & Servanty, S. The influence of landscape structure on female roe deer home-  
783 range size. *Landsc. Ecol.* **20**, 1003–1012 (2005).
- 784 54. Van Moorter, B., Visscher, D., Herfindal, I., Basille, M. & Mysterud, A. Inferring  
785 behavioural mechanisms in habitat selection studies getting the null-hypothesis right for  
786 functional and familiarity responses. *Ecography (Cop.)*. **36**, 323–330 (2013).
- 787 55. Morales, J. M. *et al.* Building the bridge between animal movement and population  
788 dynamics. *Philos. Trans. R. Soc. B Biol. Sci.* **365**, 2289–2301 (2010).
- 789 56. Hooten, M. B., Scharf, H. R. & Morales, J. M. Running on empty: recharge dynamics from  
790 animal movement data. *Ecol. Lett.* **22**, 377–389 (2019).
- 791 57. Gaillard, J. M. *et al.* Habitat-performance relationships: finding the right metric at a given  
792 spatial scale. *Philos. Trans. R. Soc. B Biol. Sci.* **365**, 2255–2265 (2010).
- 793 58. Spampinato, G., Cameriere, P., Caridi, D. & Crisafulli, A. Carta della biodiversità vegetale  
794 del Parco Nazionale dell'Aspromonte (Italia meridionale). *Quad. di Bot. Ambient. e Appl.*  
795 **19**, 3–36 (2008).
- 796 59. Fortin, D. *et al.* Wolves influence elk movements: behavior shapes a trophic cascade in  
797 Yellowstone National Park. *Ecology* **86**, 1320–1330 (2005).
- 798 60. European Environment Agency. European digital elevation model (EU-DEM), version 1.0.  
799 (2016). Available at: <https://land.copernicus.eu/imagery-in-situ/eu-dem/eu-dem-v1-0-and->



- 800 derived-products. (Accessed: 23rd February 2018)
- 801 61. European Environment Agency. Tree Cover Density, Copernicus Land Monitoring  
802 Service. (2012). Available at: [https://land.copernicus.eu/pan-european/high-resolution-](https://land.copernicus.eu/pan-european/high-resolution-layers/forests/tree-cover-density)  
803 [layers/forests/tree-cover-density](https://land.copernicus.eu/pan-european/high-resolution-layers/forests/tree-cover-density). (Accessed: 23rd February 2018)
- 804 62. European Environment Agency. CORINE Land Cover. (2012). Available at:  
805 <https://land.copernicus.eu/pan-european/corine-land-cover>. (Accessed: 18th May 2015)
- 806 63. Morales, J. M., Haydon, D. T., Frair, J., Holsinger, K. E. & Fryxell, J. M. Extracting more  
807 out of relocation data: Building movement models as mixtures of random walks. *Ecology*  
808 **85**, 2436–2445 (2004).
- 809 64. Manly, B. F., McDonald, L., Thomas, D., McDonald, T. L. & Erickson, W. P. *Resource*  
810 *selection by animals. Statistical design and analysis for field studies*. (Springer-Verlag  
811 New York Inc., 2002).
- 812 65. Ziegler, P. E. & Wehner, R. Time-courses of memory decay in vector-based and  
813 landmark-based systems of navigation in desert ants, *Cataglyphis fortis*. *J. Comp. Physiol.*  
814 **181**, 13–20 (1997).
- 815 66. White, K. G. Forgetting functions. *Anim. Learn. Behav.* **29**, 193–207 (2001).
- 816 67. Poli, R., Kennedy, J. & Blackwell, T. Particle swarm optimization. An overview. *Swarm*  
817 *Intell.* **1**, 33–57 (2007).
- 818 68. Akaike, H. Information theory and an extension of the maximum likelihood principle. in  
819 *Proceedings of the 2nd International Symposium on Information Theory* (eds. Petrov, B.  
820 N. & Csaki, F.) 267–281 (Budapest: Akademiai Kiado, 1973).
- 821 69. Sharma, G. & Martin, J. MATLAB®: a language for parallel computing. *Int. J. Parallel*  
822 *Program.* **37**, 3–36 (2009).
- 823 70. R Development Core Team. R: a language and environment for statistical computing. R

824 Foundation for Statistical Computing, Vienna, Austria. [www.r-project.org](http://www.r-project.org). (2016).

825